Preprints.org

Article

Evaluation of the Ability of Wasp Venom Bioinspired Peptides (Fraternine-10 and Octovespin) in the Disaggregation and Anti-aggregation of Amyloid-β and α-Synuclein Fibrils

Yuri Alves de Oliveira Só , Caio Vinícius Sousa Costa , Luana Cristina Camargo , Letícia Germino Veras , Luiz Antônio Ribeiro Júnior , Márcia Renata Mortari , And Ricardo Gargano *

Article

Evaluation of the Ability of Wasp Venom Bioinspired Peptides (Fraternine-10 and Octovespin) in the Disaggregation and Anti-aggregation of Amyloid-β and α-Synuclein Fibrils

Yuri Alves de Oliveira Só [1], Caio Vinícius Sousa Costa [1], Luana Cristina Camargo [2], Letícia Germino Veras [2], Luiz Antônio Ribeiro Júnior [1], Márcia Renata Mortari [2] and Ricardo Gargano [1,*

[1] Institute of Physics, University of Brasilia, Brasilia, Brazil; yurialves.y@gmail.com (Y.A.d.O.); caio.vinicius3215@gmail.com (C.V.S.C.); ribeirojrfis@gmail.com (L.A.R.J.)

[2] Laboratory of Neuropharmacology, Department of Physiological Sciences, University of Brasilia, Brasilia, Brazil; luana.camargo@unb.br (L.C.C.); leticiagveras@gmail.com (L.G.V.); mmortari@unb.br (M.R.M.)

* Correspondence: gargano@unb.br

Abstract: Many neurodegenerative diseases are directly related to the formation of toxic protein aggregates, such as Parkinson's and Alzheimer's diseases, which are associated with the aggregation of alpha-synuclein (α-syn) and beta-amyloid (Aβ), respectively. In this context, protein fibrils are the hallmark of these neurodegenerative diseases. In this sense, planning or designing compounds that are capable of preventing or reducing the formation of protein aggregation in the brain can be of fundamental importance for the curative treatment of these diseases. This work presents an *in silico* and experimental study to investigate the inhibitory potential of the ligands Octovespin (bioinspired by the wasp venom *Polybia Occidentalis*) and Fraternine-10 (bioinspired by the wasp venom *Parachartergus fraternus* wasp) against the aggregation of fibrils of the peptides Aβ(17-42) and α-syn, respectively. Using molecular docking and molecular dynamics simulations with 100 ns, the disaggregation capacity of these ligands was studied. The results obtained indicate that Octovespin and Fraternine-10 interact with the Aβ and α-syn protein fibrils throughout the simulation time. The RMSD values and the interactions with amino acids responsible for fibril aggregation demonstrate that both Octovespin and Fraternine-10 have a significant disaggregation potential, which corroborates the observations *in vitro* and *in vivo*. Furthermore, experimental results of Fraternine-10 demonstrate an anti-aggregation effect, indicating that it can promote the disaggregation of fibrils and prevent them from aggregating again to form oligomers. These discoveries qualify these molecules as potential candidates to become medicines against Parkinson's and Alzheimer's diseases.

Keywords: wasp venom; Parkinson's disease; Alzheimer's disease; disaggregation effect; antiaggregation effect; docking molecular; dynamics molecular

1. Introduction

Alzheimer's (AD) and Parkinson's (PD) diseases are neurodegenerative disorders that are associated with the formation of insoluble protein deposits. These deposits disrupt the normal functioning of neurons, blocking neurotransmitters and leading to apoptosis. The main protein responsible for the damage in Alzheimer's disease is beta-amyloid (Aβ), which is formed from an amyloidogenic process, where two enzymes, β-secretase (BACE1) and γ-secretase, cleave the amyloid precursor protein (APP) into Aβ monomers [1,2]. These parts can aggregate to form fibrils, and then plaques. The main protein responsible for the damage in Parkinson's disease is alpha-synuclein (α-syn), which is involved in the process of storing dopamine neurotransmitter reserves. The cause of its aggregation is still unknown. Scientific evidence points to the centrality of α-syn, an intrinsically disordered protein in the cytosol that is considered to be essential for the development of the disease. The etiology of PD is varied, and depending on the triggering factor of the pathology, several changes can occur in the physiological pathways and the monomer α-syn. Changes in the protein can lead to damage to cellular pathways,

and damage to these pathways can also cause changes in the protein. Ultimately, neuronal death occurs, and in resilient neurons, Lewy bodies composed mainly of α-syn are found. These bodies are formed because, in an initial phase, changes in cellular homeostasis induce disturbances in the equilibrium between the different forms of α-syn, originating in the formation of toxic oligomers and fibrils. In addition to the damage they cause to cellular pathways, these species can spread in a prion-like manner, interfering with the homeostasis of neighboring cells. It is believed that their accumulation is due to combinations of genetic (mutations in Park1) and environmental factors, which can reduce the ability of this protein to cleave α-syn [3–5].

The most common Aβ filaments found in AD are peptides of 38-43 amino acids, with the Aβ(1-42) and Aβ(1-40) forms being the most common. Aggregation depends primarily on the hydrophobic amino acid portion, which, due to this property, makes it prone to clumping together, forming a hydrophobic structure. This portion represents the amino acids from 16-20, consisting of Lysine 16 (K), Leucine 17 (L), Valine 18 (V), Phenylalanine 19 (F), and Phenylalanine 20 (F), and from 39-42, consisting of Valine 39 (V), Valine 40 (V), Isoleucine 41 (Ile), and Alanine (42). The latter is known as the hydrophobic C-terminus. The most common α-syn filaments found in PD are peptides of 121 amino acids. The main amino acids, also hydrophobic, responsible for the stability of the α-syn protofilaments are those from 50-57, found in the interface region between two α-syn fibrils. These are Histidine (50), Glycine (51), Valine (52), Alanine (53), Threonine (54), Valine (55), Alanine (56), and Glutamate (57).

Finding drugs that promote the disaggregation of Aβ and α-syn is as important as obtaining drugs that can act as antiaggregators, since oligomers, which are smaller aggregates of these proteins, are even more toxic than fibrils [6]. Oligomers can penetrate cells and cause more damage than fibrils [7,8]. Therefore, it is important to develop therapies that can disaggregate fibrils and prevent them from re-aggregating into oligomers. Based on this knowledge, some research groups have developed some experimental and computational strategies to find inhibitors that can block the aggregation process, intervene in metal complexation, or even induce the disaggregation of Aβ and α-syn fibrils [9–12].

Following these same steps, our research group has been investigating the properties of some peptides derived from wasp venom intending to find a compound that can inhibit the action of the peptides Aβ and α-syn. Among them, we chose to investigate the derivatives of the venom of the wasps *Polybia occidentalis* and *Parachartergus fraternus*. From the first, it was obtained the compound called Fraternine-10 [13,14] and, from the second, Octovespin [15]. The molecular structure of Octovespin and Fraternine-10 is presented in Figure 1, Fraternine-10 has the peptide sequence: Leu-Ser-Phe-Gln-Lys-Val-Lys-Glu-Lys-Val-NH2, and Octovespin: Gln-Met-Trp-Ala-Val-Phe-Trp-Met-NH2. Fraternine-10 showed a relative antiparkinsonian effect in a model of neurodegeneration in mice [16]. *In vitro* assays showed that Octovespin decreased the aggregation of Aβ fibrils, and *in vivo* assays in mice demonstrated the ability of this compound to prevent the aggregation of Aβ and reduce induced negative cognitive effects [17]. No information on Fraternine-10 efficacy as an anti-aggregator to Aβ and α-syn is available at the moment.

Based on these reports, the present work aims to investigate, using computational methods, the properties and capabilities of the peptides Octovespin and Fraternine-10 to promote the disaggregation of the fibrils of Aβ and α-syn. To this end, molecular docking and molecular dynamics techniques were used using Aβ(18-42) and α-syn(38-95) fibrils as targets. Additionally, experimental results of Fraternine-10 are presented regarding its ability to prevent or delay the formation of oligomers that may be formed after the disaggregation of fibrils, to complement the results obtained computationally.
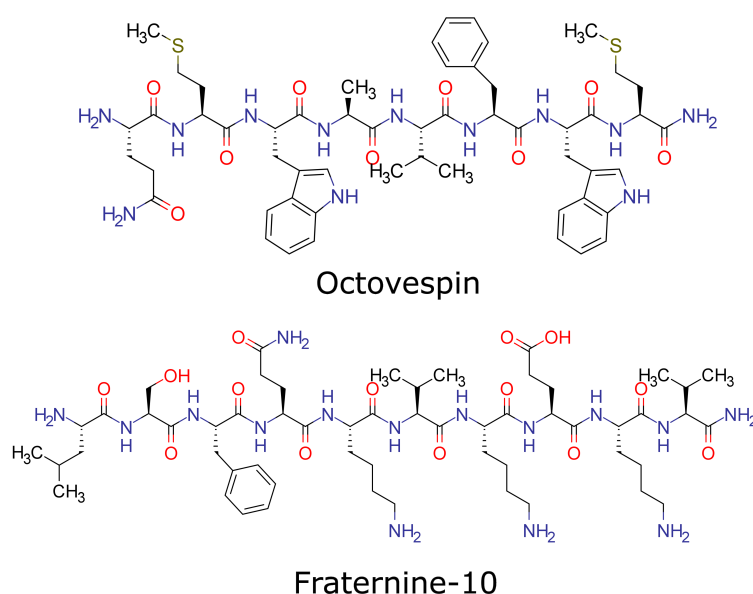
Figure 1. Molecular structure of Octovespin and Fraternine-10.

1.1. Target Proteins

To carry out this study, the proteins Aβ and α-syn (represented in the form of fibrils) were considered as targets, as shown in Figure 2. For beta-amyloid, the structure with PDB ID: 2BEG was chosen, which is a 3D structure of Aβ(18-42) fibrils determined by Luhrs et al. [18] in 2005 using solid-state nuclear magnetic resonance spectroscopy. The fibrils are composed of five twisted beta sheets, named A, B, C, D, E, and F, with the Aβ(18-42) peptides stacked on top of each other in a ladder-like fashion. The beta sheets are stabilized by a network of hydrogen bonds and hydrophobic interactions. The fibrils are highly polymorphic, meaning that they can exist in different shapes and sizes. However, all fibrils share the same basic structure of twisted beta sheets.
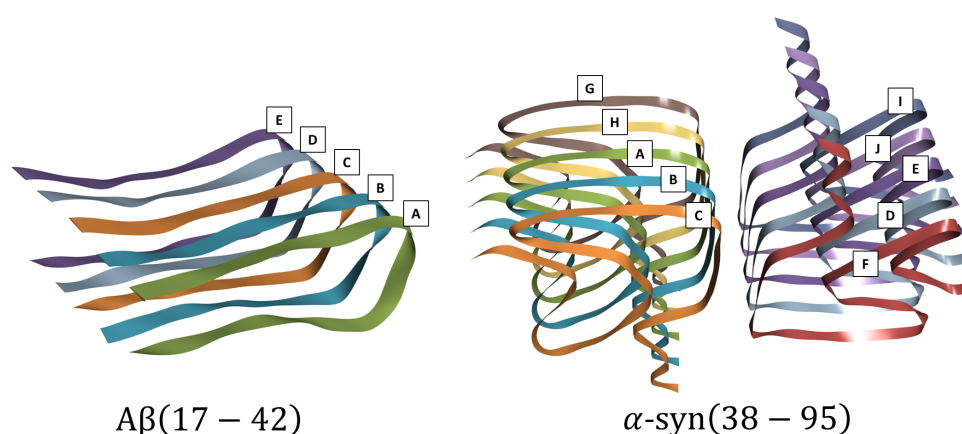

Figure 2. Aβ(17-42) (left), PDB ID: 2BEG, and α-syn(38-95) (right), PDB ID: 6H6B, with the designation of their respective sheets.

For α-syn, the structure with PDB ID: 6H6B was chosen, which is a 3D structure of α-syn(38-95) fibrils determined by Guerrero-Ferreira et al. [19] in 2005 using cryo-electron microscopy. This structure shows that α-syn(38-95) fibrils are formed by a parallel arrangement of two sets of beta sheets. The beta sheets are composed of long, thin protein filaments arranged in a zigzag pattern. The chains are held together by hydrogen bonds, which are weak bonds that form between oxygen atoms in the protein structure. The beta sheets are stacked on top of each other and the strands of one sheet run

perpendicular to the strands of the next sheet. One set is named by the sequence of sheets C, B, A, H, and G, and the other by the sequence F, D, E, J, and I.

2. Methodology

2.1. Computational Details

The structures and calculations used in this study were prepared as follows. The structures of the Aβ(17-42) and α-syn(38-95) fibrils were obtained from the Protein Data Bank (https://www.rcsb.org/). For molecular docking, the protonation states of each ligand were adjusted to pH 7.4 and all histidine residues were protonated using the PlayMolecule-ProteinPrepare server [20]. Missing hydrogen atoms were added and the binding site was defined as the entire peptide to investigate all possible binding modes. Molecular docking was performed using the Autodock Vina computational package [21], implemented in PyRx [22], using the genetic algorithm as the default configuration. The population size was set to 100. The center of the box was defined as the center of the fibril and docking was performed on the entire fibril. The conformations were selected according to the binding affinity and the region of interest, selecting the configurations where the peptides docked at or close to the fibril aggregation interface. The visual analysis results and production of contact maps was performed using the ChimeraX [23,24] and Discovery Studio 2016 [25] programs. The molecular dynamics inputs were built using the online Chemistry at Harvard Macromolecular Mechanics (CHARMM-GUI) program [26,27] and the dynamics calculations were performed using the Nanoscale Molecular Dynamics (NAMD) 2.9 program [28]. The parameterization of the peptides was performed using the online SwissParam program [29]. The dynamics box was defined as being 120 Å x 100 Å x 100 Å. To simulate the solvent, the TIP3P water model [30] was used and the appropriate number of sodium and chloride ions were added to neutralize the system and reach physiological pH conditions equal to a concentration of 0.15 NaCl. Molecular dynamics was performed in two stages, the first of equilibration, with a time of 10 ns, and the second of production, with a time of 100 ns, both with a timestep of 1.0 fs. Periodic boundary conditions were imposed via the Particle Mesh Ewald (PME) full electrostatics method and NVT and NPT ensemble with pressure equal to 1013.25 hPa and temperature of 300 K using Langevin dynamics to control the temperature. The visual analysis of the results was performed using the Visual Molecular Dynamics (VMD) 1.9.1 program [31]. The simulation systems were built from the complexes with ligands obtained from the docking and the isolated proteins.

2.2. Thioflavin T (ThT) Assay

Aβ(1–42) (Biointech, Brazil) was prepared following the method outlined by Camargo et al. [17]. For the ThT assay, a 96-well plate with a dark surface was utilized, containing 50 μL of the Aβ(1–42) solution (75 μM), 50 μL of ThT, 50 μL of Fraternine-10 at three different concentrations (75, 37.5, and 18.8 μM). The kinetic readings were performed in a plate reader (Varioskan LUX Multimode Microplate Reader) with an excitation wavelength of 450 nm and emission wavelength of 490 nm, at 37 °C, with readings taken every 5 min over 24h. The entire procedure was carried out in a dark environment to avoid interference with ThT fluorescence and was done in three independent experiments.

3. Results and Discussion

The results of the molecular docking showed that Octovespin and Fraternine-10 bind to the same region of both Aβ(17-42) and α-syn(38-95) fibrils, as shown in Figure 3. In the case of Aβ(17-42), the ligands docked along the axis of the fibril between one of the lateral fragments of the β- sheet. Fraternine-10 docked along the axis of the fibril with the lateral fragment of the A sheet of the fibril in the most central part, interacting with the amino acids Leu17(A), Leu34(A), Phe19(A), Phe20(A), Gly25(A), Gly38(A), Glu22(A), Asp23(A), and Val24(A). Octovespin docked in a similar region, but shifted towards the edge of the A filament, with interactions with the A, B, and C sheets, and interacting with the amino acids Asp23(A), Ala21(A), Val18(A), Val36(A), Phe20(A), Ala21(B), Leu34(B), Val36(B),

and Val36(C). The score function, which measures the binding affinity, of the docking of Aβ(17-42) with Fraternine-10 had a value of -5.1 kcal/mol and that of Octovespin of -6.2 kcal/mol. In the case of α-syn(38-95), both ligands docked near the region of interaction between the two sets of fibrils, in one of the pockets, near the intersection region of the set of fibrils, formed by the sheets C, B, A, H, and G. Fraternine-10 showed interaction with the amino acids Lys60(C), Thr59(C), Val63(C), Glu61(C), Gly73(C), Val63(C), Ala56(B), Glu61(B), Thr72(B), Gly73(B), Thr75(B), Gly73(A), Thr75(A), Glu61(A), Thr59(A), Thr59(H), Glu61(H), Val55(H), and Gly73(H). Octovespin showed interaction with the amino acids Gly73(C), Thr59(C), Glu61(C), Thr75(B), Gly73(B), Ala56(B), Thr59(B), Thr75(A), Thr75(H), Thr59(H), Ala56(H), and Glu61(H). The score function, which measures the binding affinity, of the docking of α-syn(38-95) with Fraternine-10 had a value of -6.4 kcal/mol and that of Octovespin of -7.9 kcal/mol.
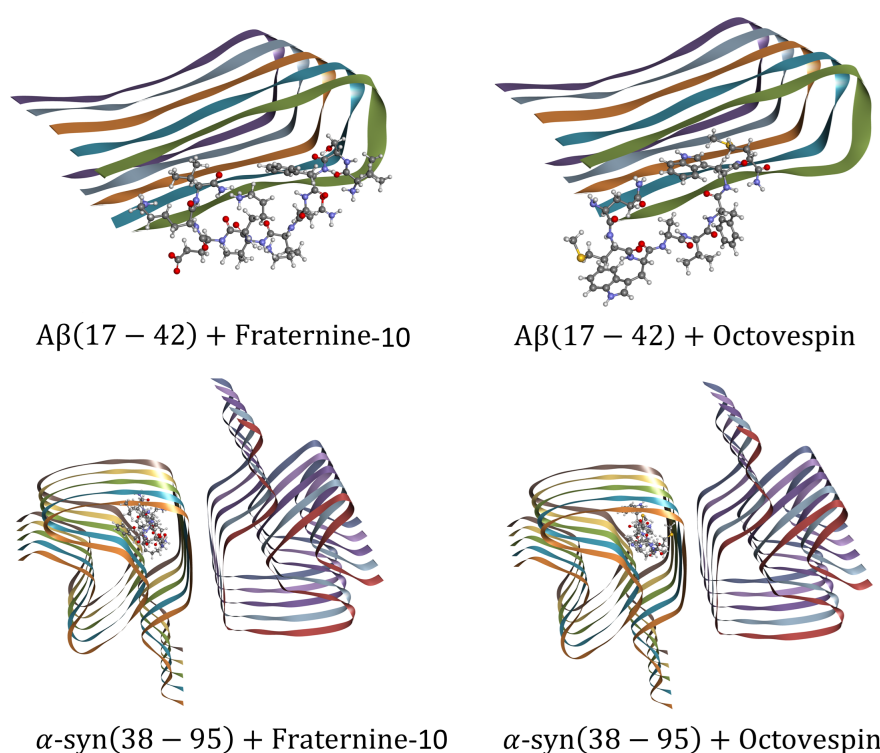

$A\beta(17-42)$ + Fraternine-10 $A\beta(17-42)$ + Octovespin

α-syn$(38-95)$ + Fraternine-10 α-syn$(38-95)$ + Octovespin

Figure 3. Best pose of the molecular docking of Fraternine-10 and Octovespin with Aβ(17-42) fibrils (PDB ID: 2BEG) (above) and α-syn(38-95) (PDB ID: 6H6B) (below).

Subsequently, molecular dynamics simulations were performed to understand how Fraternine-10 and Octovespin interact with the target fibrils. The changes in secondary structure were analyzed during the dynamic simulation for complexes of each compound, as well as for isolated target fibrils. Differences were observed in the conformation of the fibrils in the presence of the compounds, mainly about the Aβ(17-42) fibril. The conformational changes are presented visually in Figures 4 and 5, with poses of the isolated fibrils and in the presence of the compounds at times of 0ns, 50ns, and 100ns of simulation.
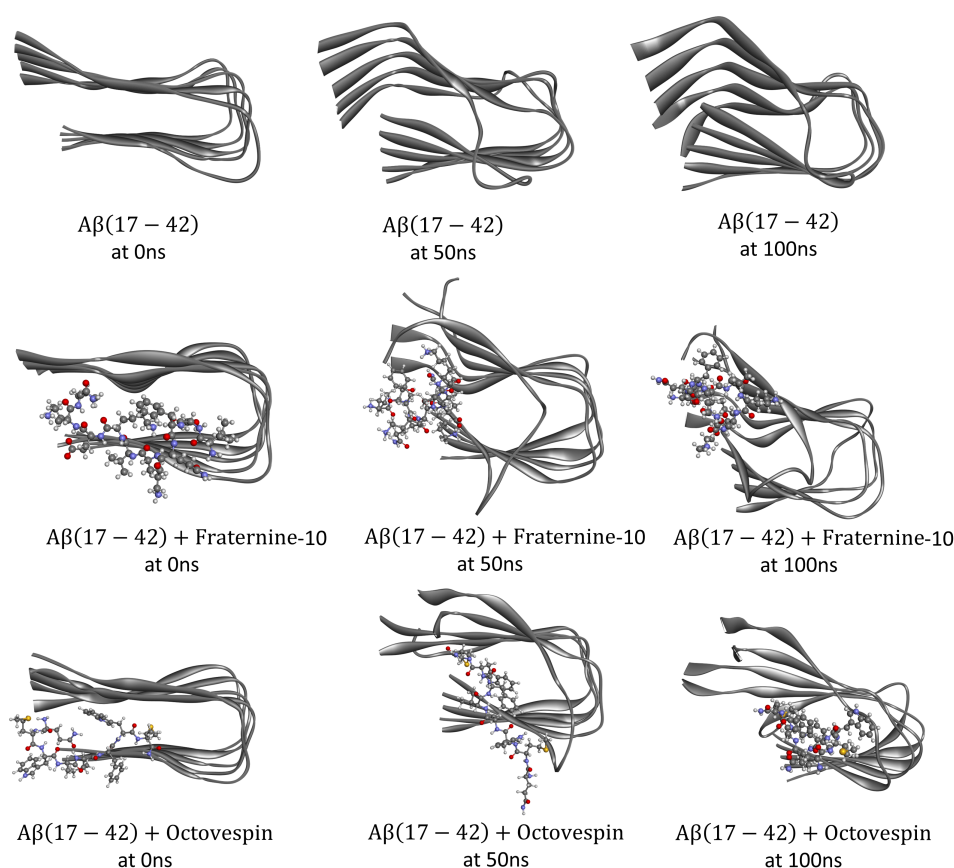
Figure 4. Conformations of the Aβ(17-42) fibril (PDB ID: 2BEG) isolated (top panel) and with Fraternine-10 (middle panel) and Octovespin (bottom panel) at times of 0 ns, 50 ns, and 100 ns.

Based on these results, the root-mean-square deviation (RMSD) of the fibrils was calculated to understand how the structural changes occurred concerning the initial conformation. Numerically, the average RMSD values obtained were 4.536Å for Aβ(17-42) alone, 5.661Å for Aβ(17-42) with Fraternine-10, 4.906Å for Aβ(17-42) with Octovespin, 2.823Å for α-syn(38-95) alone, 2.834Å for α-syn(38-95) with Fraternine-10, and 3.663Å for α-syn(38-95) with Octovespin. For the Aβ(17-42) fibril, the interaction with Fraternine-10 showed considerable changes in the first 20 ns of simulation, decreasing the RMSD value after that time and up to 100 ns. Between 60-70 ns there was an increase in the peak, as shown in Figure 6. With the interaction with Octovespin, small conformational changes occurred until approximately 85 ns, where from that moment, the RMSD showed a sharp trend of increasing in its value, indicating a greater change in the conformation of the fibril after that time. About the α-syn(38-95) fibril, the RMSD of the fibril alone and in the presence of the compounds showed small variations, but with emphasis on its value when in the presence of Octovespin, which showed a more considerable change in the RMSD. This is because α-syn(38-95) fibrils are relatively larger than Aβ(17-42) fibrils and, therefore, have less mobility and greater resistance to conformational change. In addition to RMSD, the number of hydrogen bonds in the intermolecular structure of the fibrils was also calculated, presented employing the graph in Figure 6. According to what was observed, for the Aβ(17-42) fibril, the decrease in bonds is noticeable in the presence of Fraternine-10, mainly after approximately 60 ns of simulation, indicating a disaggregating effect of this compound. To the α-syn(38-95) fibril, there can also be noted a decrease in the number of hydrogen bonds in the intermolecular structure, mainly around 80 ns and after, but in smaller quantity.
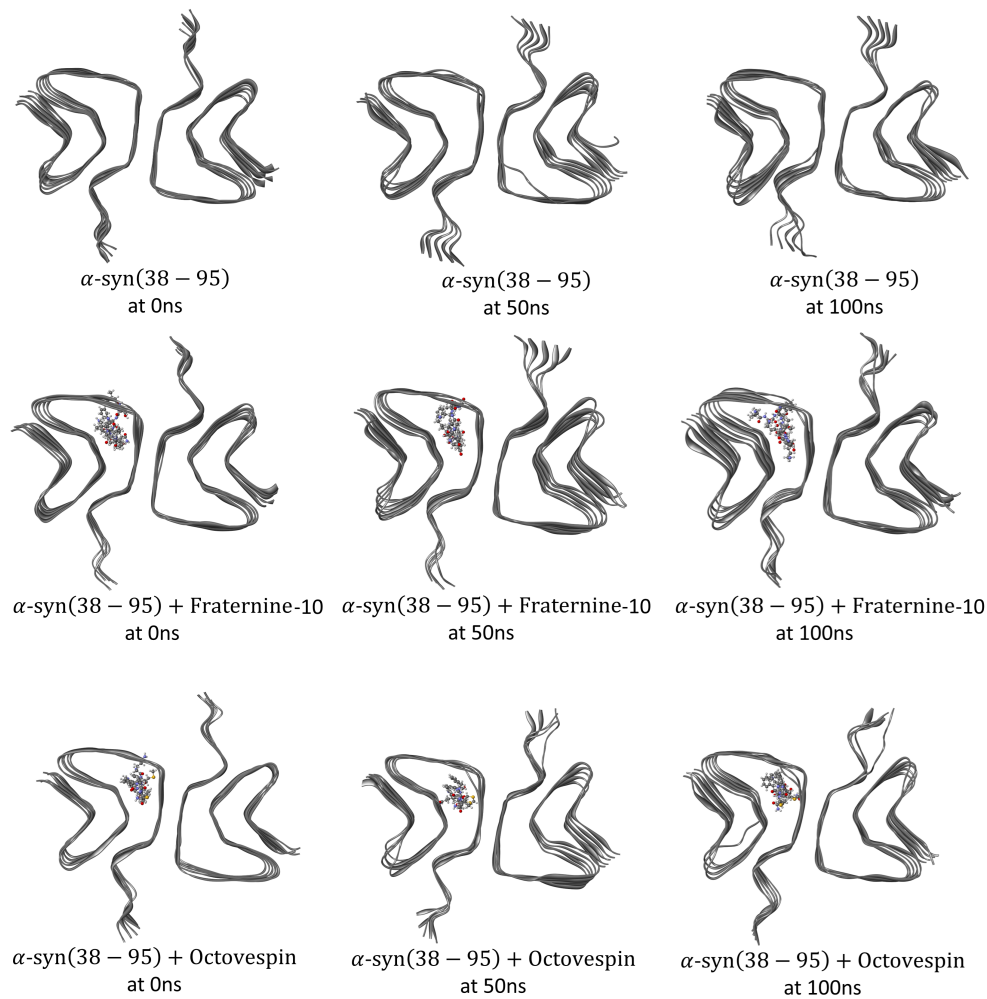
Figure 5. Conformations of the α-syn(38-95) fibril (PDB ID: 6H6B) isolated (top panel) and with Fraternine-10 (middle panel) and Octovespin (bottom panel) at times of 0 ns, 50 ns, and 100 ns.

The root-mean-square fluctuation (RMSF) of the fibrils was also calculated in order to understand how the change in the flexibility of the fibrils occurs in the presence of peptides. The obtained results are shown in Figure 6. For Aβ(17-42) fibrils, residues 1-26 represent the A sheet, 27-52 the B sheet, 53-78 the C sheet, 79-104 the D sheet, and 105-130 the E sheet. The results indicate a increase in fibril flexibility in the presence of Fraternine-10, with RMSF peaks pronounced close to the central region of the fibril cavity. For Octovespin, the results indicated little change in the flexibility of the fibril, following the same behavior of the isolated fibril. For α-syn(38-95) fibrils, residues 1-58 represent the C sheet, 59-116 the B sheet, 117-174 the A sheet, 175-232 the H sheet, 233-290 the sheet G, 291-348 the F sheet, 349-406 the D sheet, 407-464 the E sheet, 465-522 the J sheet, and 523-580 the I sheet. Our findings suggest that both peptides slightly influence the flexibility of α-syn(38-95). Notably, Octovespin exhibited a more pronounced effect, transiently increasing the fibrils RMSF close to the interface region during the simulation.
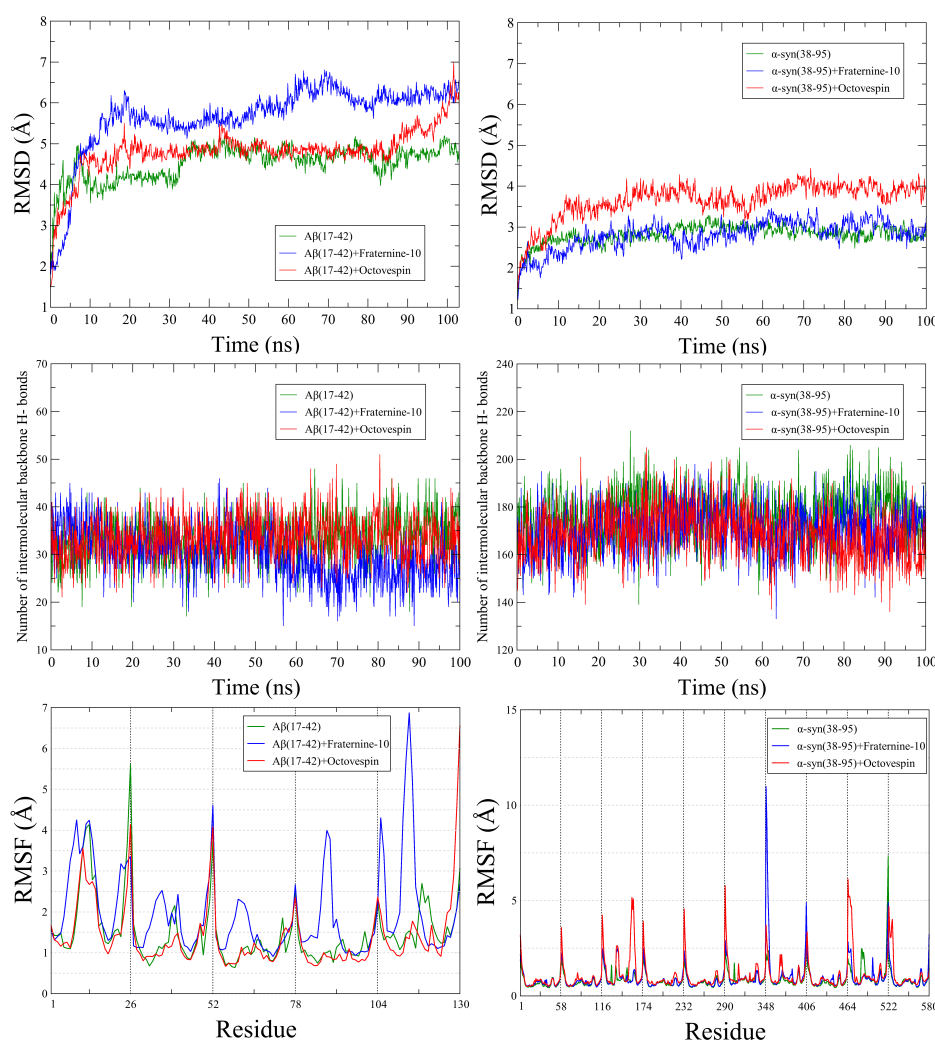
Figure 6. Root-mean-square deviation (RMSD) (top) and evolution of the number of hydrogen bonds in the intermolecular structure (mid), and root-mean-square fluctuations (RMSF) (down) for the isolated Aβ(17-42) fibril (green, left), isolated α-syn(38-95) fibril (green, right), and fibrils with Fraternine-10 (blue) and Octovespin (red).

Subsequently, an analysis of the interactions of the compounds with Aβ(17-42) and α-syn(38-95) fibrils at 0, 50, and 100 ns of the simulation was performed, the interactions of which are presented in Figures 7 and 8. For Fraternine-10 and Aβ(17-42), during the 100 ns of simulation, the interactions occurred primarily with the amino acids Val36 (π-alkyl), Ala21 (hydrogen bond) and Leu17 (hydrogen bond). It is worth noting that a large part of the interactions also occurred with the amino acids Val39 (π-alkyl) and Val40 (π-alkyl), which are amino acids responsible for the aggregation of Aβ(17-42) fibrils. Concerning Fraternine-10 and α-syn(38-95), during the 100 ns of simulation, the interactions occur primarily with the amino acids Thr59 (hydrogen bond), Glu61 (π-anion) and Gly73 (carbon hydrogen bond). To Octovespin and Aβ(17-42) during the 100 ns of simulation, the interactions occurred primarily with the amino acid Phe19 (hydrogen bond). For Octovespin and α-syn(38-95), during the 100 ns of simulation, the interactions occurred primarily with the amino acids Ala56 (π-alkyl) and Thr75 (hydrogen bond). It is worth noting that a large part of the interactions occurred with the amino acid Ala56 (π-alkyl) which is one of the amino acids responsible for the aggregation of α-syn fibrils.
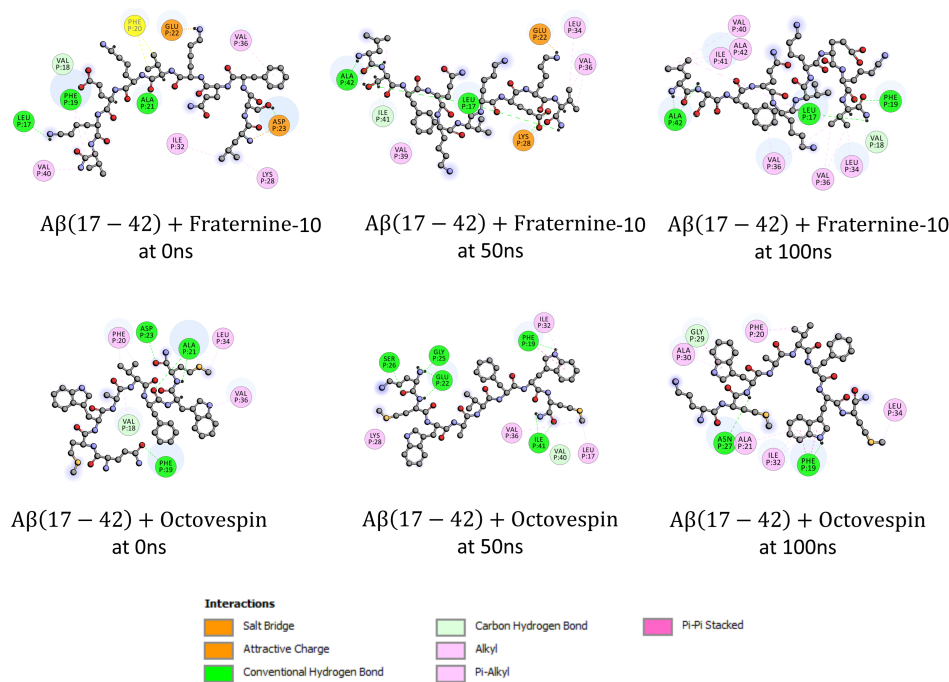
Figure 7. Amino acids in the Aβ(17-42) fibril that interact with Fraternine-10 and Octovespin at 0 ns, 50 ns, and 100 ns of simulation.
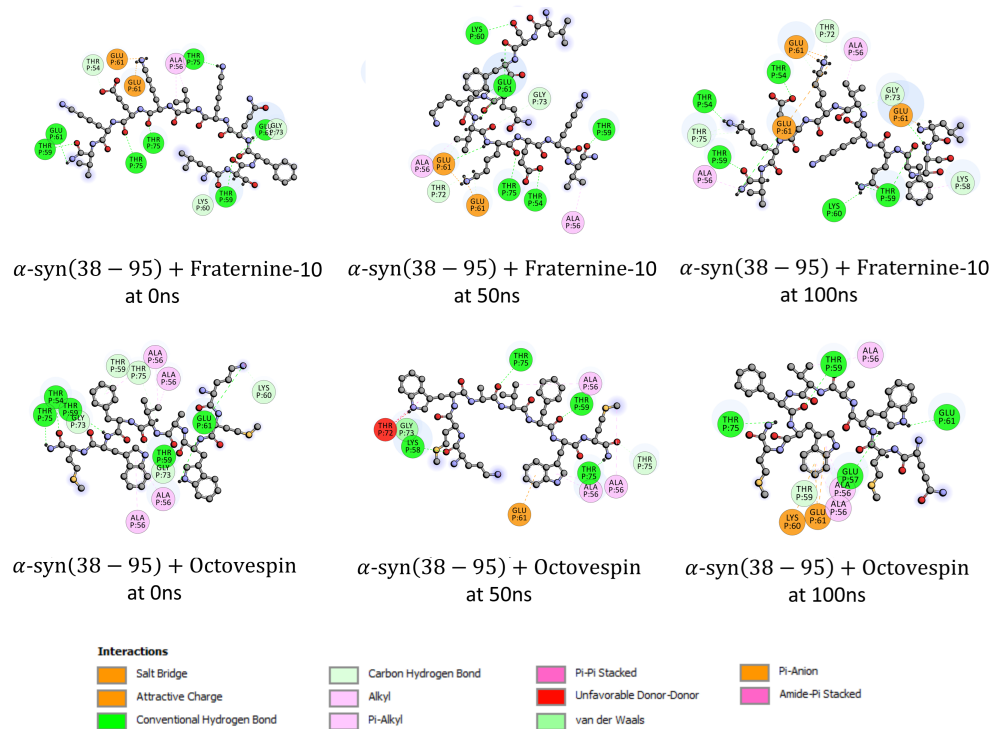

Figure 8. Amino acids in the β-syn(38-95) fibril that interact with Fraternine-10 and Octovespin at 0 ns, 50 ns, and 100 ns of simulation.

Considering the ThT assay, Fraternine-10 intermediate (37.5 μM) and low dose (18.8 μM) had ThT signal decrease compared to Aβ(1-42) alone (two-way ANOVA; F (864, 9216) = 2.048; p<0.0001), as shown in Figure 9. However, the signal started to increase after 12h which indicated the ability of Fraternine-10 to delay amyloid aggregation but not to prevent it. Finally, Fraternine-10 high dose (75

μM) did not affect amyloid aggregation. According to Camargo and collaborators [17], Octovespin also prevented amyloid aggregation in the ThT assay.
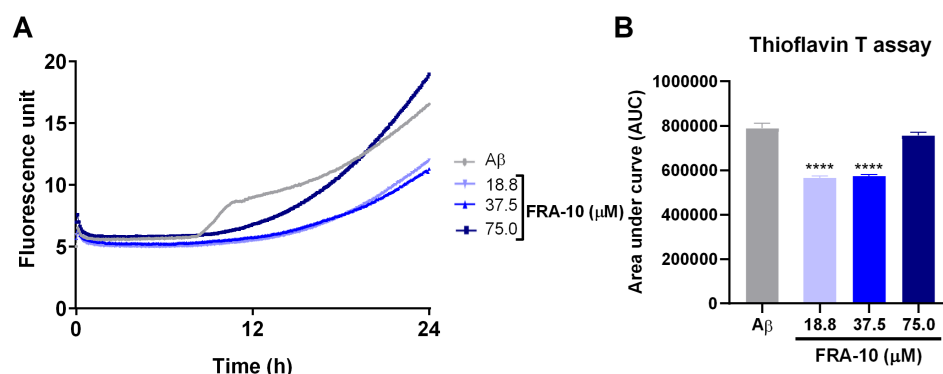

Figure 9. The Fraternine-10 efficacy in preventing Aβ aggregation *in vitro*. Three doses of Fraternine-10 (75, 37.5, and 18.8 μM) were evaluated. In A, anti-aggregating effect in the kinetics measurement for 24h. In B, the Area under the curve (AUC) of the anti-aggregating effect. Two-way ANOVA followed by Tukey test: ****p < 0.0001: Aβ compared to Fraternine-10 doses.

Certain natural peptides also showed promising results both *in silico* and *in vitro* in the Aβ aggregation. Carnosine, a peptide naturally produced in muscles and brain, has demonstrated a reduction in the formation of Aβ fibrils, as evidenced by atomic force microscopy (AFM) and the ThT assay. Moreover, *in silico* data showed that carnosine and homocarnosine interact in D23 and K28 of the Aβ sequence, which are amino acid residues involved in the self-association process [32,33].

While several peptides have been specifically designed to prevent amyloid aggregation, a category called "β-sheet breakers" had limitations throughout the drug development. Synthetic pseudo-peptides with around 8 amino acid residues (Sg inhibitor) were designed to bind in the aggregation-prone region Aβ(16–23). The evaluation of MD simulations showed that SGC1 had more favorable binding to Aβ although demonstrated inefficacy against Aβ toxicity in cells. Interestingly, other peptides with less favorable binding had a better protective effect [34]. In the present study, both Fraternine-10 and octovespin showed good binding to Aβ and were effective in the ThT assay and in vivo [17]. Similar to fraternine-10, a dipeptide D-Trp-Aib showed also promising results in the MD simulation and probable interaction with Lis17 and Phe19 of Aβ hydrophobic core [35].

Regarding *in silico* assessment of peptide interactions with α-syn, only a limited number of studies are available. Other molecules have been studied, such as Copper (Cu (II)). Cu(II) binds to α-syn seems to increase conformation stability [36]. For instance, a study showed that 5,7-dihydroxy-2-[(2R,3R)-3-(hydroxymethyl)-2-(4-hydroxyphenyl)-2,3-dihydro-1,4-benzodioxin-6-yl]chromen-4-one can alter α-syn conformation by molecular dynamics evaluation and interaction with Glu57 [37]. Similarly, derivatives of 7,8-Dihydroxyflavone had high binding affinity and interacted with Gln99, Ala90, Ser87, Val95, Gly93, Leu100 and Lys97 amoung other amino acids residues [38]. In the present study, the impact of Octovespin and Fraternine-10 on α-syn conformation was assessed through RMSD and molecular dynamics. Octovespin induced conformational changes and exhibited interactions with Ala56 and Thr75 amino acid residues. Fraternine-10, on the other hand, induced subtle changes in α-synuclein conformation and interacted with Thr59, Glu61, and Gly73. In summary, both Octovespin and Fraternine-10 demonstrated good interaction with α-syn and Aβ, which shows their potential as compounds of interest in further exploration and development.

4. Conclusion

Molecular docking applications, followed by dynamic simulations, allowed estimating the potential activity of Octovespin and Fraternine-10 peptides in inhibiting the aggregation of beta-amyloid and alpha-synuclein. Both ligands showed π-alkyl interactions with the amino acids responsible for aggregation and fibril formation. More specifically, Fraternine-10 interacts with Val39 and Val40 of

Aβ(17-42) and Octovespin with Ala56 of α-sin(38-95) and, when disruptive, these interactions can disaggregate the fibrils. Furthermore, the hydrogen bonds of the intermolecular structure Aβ(17-42) with Fraternine-10 showed a relative decrease in 100 ns of simulation and also with Octovespin after 90 ns. Regarding hydrogen bonds in the intermolecular structure of α-syn(38-95), Octovespin was the most notable, with the greatest relative decrease over the 100 ns of simulation. Based on RMSD and RMSF analyses, Fraternine-10 exhibited better potential to disaggregate the Aβ(17-42) fibrils, while Octovespina showed better potential to disaggregate the α-syn(38-95) fibrils.

These computational simulations corroborate with the experimental results, that is, the Octovespin can prevent the aggregation and the Fraternine-10 can delay the aggregation of Aβ oligomers. These findings are very important because they suggest that these peptides may have the ability to disaggregate fibrils and may delay or prevent post-oligomer formation.

The *in silico* analysis procedures adopted in this study, together with the experimental results, can help in the search for new compounds that prevent the aggregation of the Aβ and α-syn peptides. Furthermore, they may also be useful to design new peptides derived from wasp venom (*Polybia occidentalis* and *Parachartergus fraternus*) to act as inhibitors of aggregating proteins such as Aβ and α-syn.

References

1. Ahmad, S.S.; Khan, S.; Kamal, M.A.; Wasi, U. The Structure and Function of α, β and γ-Secretase as Therapeutic Target Enzymes in the Development of Alzheimer's Disease: A Review. *CNS & Neurological Disorders-Drug Targets (Formerly Current Drug Targets-CNS & Neurological Disorders)* **2019**, *18*, 657–667.

2. Schaduangrat, N.; Prachayasittikul, V.; Choomwattana, S.; Wongchitrat, P.; Phopin, K.; Suwanjang, W.; Malik, A.A.; Vincent, B.; Nantasenamat, C. Multidisciplinary approaches for targeting the secretase protein family as a therapeutic route for Alzheimer's disease. *Medicinal Research Reviews* **2019**, *39*, 1730–1778.

3. Li, W.; Fu, Y.; Halliday, G.M.; Sue, C.M. PARK genes link mitochondrial dysfunction and alpha-synuclein pathology in sporadic Parkinson's disease. *Frontiers in Cell and Developmental Biology* **2021**, *9*, 612476.

4. Kim, S.; Pajarillo, E.; Nyarko-Danquah, I.; Aschner, M.; Lee, E. Role of Astrocytes in Parkinson's Disease Associated with Genetic Mutations and Neurotoxicants. *Cells* **2023**, *12*, 622.

5. Rouaud, T.; Corbillé, A.G.; Leclair-Visonneau, L.; de Lataillade, A.d.G.; Lionnet, A.; Preterre, C.; Damier, P.; Derkinderen, P. Pathophysiology of Parkinson's disease: Mitochondria, alpha-synuclein and much more.... *Revue Neurologique* **2021**, *177*, 260–271.

6. Verma, M.; Vats, A.; Taneja, V. Toxic species in amyloid disorders: Oligomers or mature fibrils. *Annals of Indian Academy of Neurology* **2015**, *18*, 138.

7. Siddiqi, M.K.; Majid, N.; Malik, S.; Alam, P.; Khan, R.H. Amyloid oligomers, protofibrils and fibrils. *Macromolecular Protein Complexes II: Structure and Function* **2019**, pp. 471–503.

8. Cascella, R.; Bigi, A.; Cremades, N.; Cecchi, C. Effects of oligomer toxicity, fibril toxicity and fibril spreading in synucleinopathies. *Cellular and Molecular Life Sciences* **2022**, *79*, 174.

9. SÓ, Y.A.d.O. Estudo Teórico de Moléculas Multialvo-dirigidas para o Tratamento da Doença de Alzheimer via Hipótese Metálica. Doutorado, Universidade de Brasília, Distrito Federal, 2022.

10. Bajda, M.; Filipek, S. Computational approach for the assessment of inhibitory potency against beta-amyloid aggregation. *Bioorganic & Medicinal Chemistry Letters* **2017**, *27*, 212–216.

11. Chang, W.E.; Takeda, T.; Raman, E.P.; Klimov, D.K. Molecular Dynamics Simulations of Anti-Aggregation Effect of Ibuprofen. *Biophysical Journal* **2010**, *98*, 2662–2670.

12. Raman, E.P.; Takeda, T.; Klimov, D.K. Molecular Dynamics Simulations of Ibuprofen Binding to Aβ Peptides. *Biophysical Journal* **2009**, *97*, 2070–2079.

13. Mayer, A.B. Novos analógos da Fraternina : avaliação do efeito antiparkinsoniano em modelo murino da Doença de Parkinson e identificação dos alvos farmacológicos. Doutorado, Universidade de Brasília, Distrito Federal, 2018.

14. Biolchi, A.M.; de Oliveira, D.G.R.; Amaral, H.d.O.; Campos, G.A.A.; Gonçalves, J.C.; de Souza, A.C.B.; Lima, M.R.; Silva, L.P.; Mortari, M.R. Fraternine, a novel wasp peptide, protects against motor impairments in 6-OHDA model of parkinsonism. *Toxins* **2020**, *12*, 550.

15. Camargo, L.C. Avaliação neuroprotetora do peptídeo octovespina, bioinspirado da peçonha de vespa social, em um modelo murino de Alzheimer. Mestrado, Universidade de Brasília, Distrito Federal, 2017.

16. Mayer, A.B.; de Oliveira Amaral, H.; de Oliveira, D.G.R.; Campos, G.A.A.; Ribeiro, P.G.; Fernandes, S.C.R.; de Souza, A.C.B.; de Castro, R.J.A.; Bocca, A.L.; Mortari, M.R. New fraternine analogues: Evaluation of the antiparkinsonian effect in the model of Parkinson's disease. *Neuropeptides* **2024**, *103*, 102390.

17. Camargo, L.C.; Veras, L.G.; Vaz, G.; de Souza, A.C.B.; Mortari, M.R. Octovespin, a peptide bioinspired by wasp venom, prevents cognitive deficits induced by amyloid-β in Alzheimer's disease mouse model. *Neuropeptides* **2022**, *93*, 102233.

18. Lührs, T.; Ritter, C.; Adrian, M.; Riek-Loher, D.; Bohrmann, B.; Döbeli, H.; Schubert, D.; Riek, R. 3D structure of Alzheimer's amyloid-β (1–42) fibrils. *Proceedings of the National Academy of Sciences* **2005**, *102*, 17342–17347.

19. Guerrero-Ferreira, R.; Taylor, N.M.; Mona, D.; Ringler, P.; Lauer, M.E.; Riek, R.; Britschgi, M.; Stahlberg, H. Cryo-EM structure of alpha-synuclein fibrils. *elife* **2018**, *7*, e36402.

20. Martínez-Rosell, G.; Giorgino, T.; De Fabritiis, G. PlayMolecule ProteinPrepare: a web application for protein preparation for molecular dynamics simulations. *Journal of chemical information and modeling* **2017**, *57*, 1511–1516.

21. Huey, R.; Morris, G.M.; Forli, S. Using AutoDock 4 and AutoDock vina with AutoDockTools: a tutorial. *The Scripps Research Institute Molecular Graphics Laboratory* **2012**, *10550*, 1000.

22. Pawar, R.P.; Rohane, S.H. Role of autodock vina in PyRx molecular docking. *Asian Journal of Research in Chemistry* **2021**.

23. Meng, E.C.; Goddard, T.D.; Pettersen, E.F.; Couch, G.S.; Pearson, Z.J.; Morris, J.H.; Ferrin, T.E. UCSF ChimeraX: Tools for structure building and analysis. *Protein Science* **2023**, *32*, e4792.

24. Goddard, T.D.; Huang, C.C.; Meng, E.C.; Pettersen, E.F.; Couch, G.S.; Morris, J.H.; Ferrin, T.E. UCSF ChimeraX: Meeting modern challenges in visualization and analysis. *Protein Science* **2018**, *27*, 14–25.

25. Studio, D. Dassault systemes BIOVIA, Discovery studio modelling environment, Release 4.5. *Accelrys Softw Inc* **2015**, pp. 98–104.

26. Jo, S.; Kim, T.; Iyer, V.G.; Im, W. CHARMM-GUI: a web-based graphical user interface for CHARMM. *Journal of computational chemistry* **2008**, *29*, 1859–1865.

27. Jo, S.; Cheng, X.; Lee, J.; Kim, S.; Park, S.J.; Patel, D.S.; Beaven, A.H.; Lee, K.I.; Rui, H.; Park, S.; others. CHARMM-GUI 10 years for biomolecular modeling and simulation. *Journal of computational chemistry* **2017**, *38*, 1114–1124.

28. Phillips, J.C.; Hardy, D.J.; Maia, J.D.; Stone, J.E.; Ribeiro, J.V.; Bernardi, R.C.; Buch, R.; Fiorin, G.; Hénin, J.; Jiang, W.; others. Scalable molecular dynamics on CPU and GPU architectures with NAMD. *The Journal of chemical physics* **2020**, *153*.

29. Zoete, V.; Cuendet, M.A.; Grosdidier, A.; Michielin, O. SwissParam: a fast force field generation tool for small organic molecules. *Journal of computational chemistry* **2011**, *32*, 2359–2368.

30.   Mark, P.; Nilsson, L. Structure and dynamics of the TIP3P, SPC, and SPC/E water models at 298 K. *The Journal of Physical Chemistry A* **2001**, *105*, 9954–9960.

31.   Humphrey, W.; Dalke, A.; Schulten, K. VMD: visual molecular dynamics. *Journal of molecular graphics* **1996**, *14*, 33–38.

32.   Aloisi, A.; Barca, A.; Romano, A.; Guerrieri, S.; Storelli, C.; Rinaldi, R.; Verri, T. Anti-aggregating effect of the naturally occurring dipeptide carnosine on aβ1-42 fibril formation. *PLoS One* **2013**, *8*, e68159.

33.   de Oliveira Só, Y.A.; de Abreu Silva, M.; Kiametis, A.S.; Sette, C.D.; Pereira Junior, M.L.; Ribeiro Júnior, L.A.; Gargano, R. A Multi-target Study of Natural Compounds in Preventing Neurodegenerative Disease Progression: A Computational Modeling Study. *Journal of Computational Biophysics and Chemistry* **2023**, *22*, 829–843.

34.   Robinson, M.; Lou, J.; Mehrazma, B.; Rauk, A.; Beazely, M.; Leonenko, Z. Pseudopeptide amyloid aggregation inhibitors: in silico, single molecule and cell viability studies. *International Journal of Molecular Sciences* **2021**, *22*, 1051.

35.   Mohammed, A.A.; Barale, S.S.; Kamble, S.A.; Paymal, S.B.; Sonawane, K.D. Molecular insights into the inhibition of early stages of Aβ peptide aggregation and destabilization of Alzheimer's Aβ protofibril by dipeptide D-Trp-Aib: A molecular modelling approach. *International Journal of Biological Macromolecules* **2023**, *242*, 124880.

36.   Savva, L.; Platts, J.A. How Cu(II) binding affects structure and dynamics of α-synuclein revealed by molecular dynamics simulations. *Journal of Inorganic Biochemistry* **2023**, *239*, 112068.

37.   Sahihi, M.; Gaci, F.; Navizet, I. Identification of new alpha-synuclein fibrillogenesis inhibitor using in silico structure-based virtual screening. *Journal of Molecular Graphics and Modelling* **2021**, *108*, 108010.

38.   Mohankumar, T.; Chandramohan, V.; Lalithamba, H.S.; Jayaraj, R.L.; Kumaradhas, P.; Sivanandam, M.; Hunday, G.; Vijayakumar, R.; Balakrishnan, R.; Manimaran, D.; others. Design and molecular dynamic investigations of 7, 8-dihydroxyflavone derivatives as potential neuroprotective agents against alpha-synuclein. *Scientific reports* **2020**, *10*, 599.